# Catalyst Mobility in

# Regenerative Fuel Cell Systems

**A Thesis Presented to**

**The Faculty of the Interdisciplinary Graduate Program**

**in Environmental Engineering**

**University of Houston**

**In Partial Fulfillment**

**of the Requirements for the Degree**

**Masters of Science in Environmental Engineering**

**By**

**Edward W. Miller**

**August 2000**

# Catalyst Mobility in

# Regenerative Fuel Cell Systems

Edward W. Miller

Approved:

Chairman of the Committee
Theodore G. Cleveland, Associate Professor
Civil & Environmental Engineering

Committee Members:

Deborah J. Roberts, Associate Professor
Civil & Environmental Engineering

Supramaniam Srinivasan, Research Scientist
Center for Energy and Environmental Studies
Princeton University

Charles Dalton, Associate Dean
Cullen College of Engineering

Theodore G. Cleveland, Program Director
Interdisciplinary program in Environmental Engineering

# ACKNOWLEDGMENTS

I express my appreciation to Dr. Ted Cleveland for his guidance and patience. I also thank Dr. Supramaniam Srinivasan for his encouragement and wisdom throughout the project.

# Catalyst Losses in a

# Regenerative Fuel Cell System

**An Abstract of a Thesis Presented to**

**The Faculty of the Interdisciplinary Graduate Program**

**in Environmental Engineering**

**University of Houston**

**In Partial Fulfillment**

**of the Requirements for the Degree**

**Masters of Science in Environmental Engineering**

**By**

**Edward W. Miller**

**August 2000**

# ABSTRACT

Fuel Cells are a solution to pollution, although not as profitable as chemical dilution, they represent the inclusion of an environmental substitution which allows for a larger and more profitable governmental institution.

# TABLE OF CONTENTS

# LIST OF TABLES

Table Page

# LIST OF FIGURES

Table Page

# 1.0 INTRODUCTION

Batteries can only store a finite amount of energy and historically their disposal has manufactured serious environmental hazards. Energy conversion devices, such as fuel cell, do not suffer from the finite energy limitations and are environmentally sound power systems. The fixed relatively constant energy densities and variable power density are the defining characteristics of batteries. Fuel cells operate on a comparable chemical mechanism but are not restricted to a finite amount of power, thus a fuel cell can convert chemical potential directly into electrical power with efficiencies of up to 80%.

## 1.1 Problem Statement

High efficiency regenerative fuel cell systems are the most likely candidate for long-term terrestrial and marine power production. Regenerative fuel cell systems are among the highest power density producers in world. Proton Exchange Membrane Fuel Cells (PEM fuel cell), have the added benefit of producing potable water as a by-product of power generation. The next 10 years will herald the introduction of the fuel cell vehicle on the commercial market. Automakers including, Honda, Daimler-Benz, Ford, and GM prepare to release the next generation of electric vehicles worldwide. Environmental impacts, due to traffic-related metals in road sediment, will escalate with the adoption of a hydrogen economy. Metals such as platinum and ruthenium are present as biogeochemical vectors as a result of catalytic converters and increasing automobile utilization.

The reduction of the fuel cell power output over time is a documented condition attributed to membrane degradation. An alternate explanation for power dissipation is the loss of the catalyst,

generally platinum, itself by the product water and electrode degradation. It is theorized that PEM fuel cells exhibit a "startup trait", which is responsible for performance improvements in the fuel cell and small amounts of catalyst loss. This research attempts to make a quantifiable determination of the PEM fuel cell catalyst losses and associated effects on the power output.

## 1.2 Background

Similar to a battery, fuel cells use electrochemical reactions to produce electricity. Fuel cells are best described as electrochemical engines, with no moving parts, which will operate as long as they have fuel. In comparison to a combustion engine, the fuel cell is quiet, more efficient, has no side reactions (i.e. emissions), and no vibrations. The PEM fuel cell is a polymer membrane fuel cell that utilizes hydrogen as fuel and combines with oxygen, generally from the air, to form a water molecule. Economic obstacles and a social stigmata surrounding historical hydrogen usage, the Hindenburg for example, are the basis of the technology transfer redundancy.

The cost of the fuel cell has been reduced through the development of low platinum loading electrodes and improved cell performances(dog and pony 1997). The cost, weight, and volume of the PEM fuel cell will have to undergo further reduction in order to compete with traditional combustion engines. There have been considerable advances in the PEM fuel cell field by Ballard Power Systems Inc. They have built and installed several fuel cell stacks as a power plant for a 72 Passenger Bus. Their 5 kW fuel cell stacks each weigh about 50 kg, however the completed unit weigh about 150 kg. However there are other fuel cell stacks with power outputs of 2.5 kW at a weight of 19 kg per completed unit. The higher power density is a result of new membrane technology and ultra low platinum loadings. The PEM fuel cell is the forerunner of

the fuel cell industry given they maintain the highest power density achieved by any comparable power source and operate at low temperatures, approximately 50-60°C.

### *1.2.1 History of the Fuel Cell*

The following section is a brief history of the progress in PEM fuel cell technology. The primary source of information for the next two sections was extracted from *Fuel Cell Systems* and *Surface Electrochemistry*.

In 1838 Sir Walter Grove made the reasoned invention of a fuel cell. At the time water electrolysis was a well-known process, and it occurred to Grove that if electricity could force water to separate into hydrogen and oxygen, putting $H_2$ and $O_2$ individually into contact to the electrodes may lead to the recombination of the gases into water and electricity. The fuel cell consisted of a very dilute sulfuric acid as the electrolyte; two platinum strips in inverted closed tubes, and hydrogen and oxygen were formed by electrolysis of the electrolyte. Grove reported his work and went on to produce a bank of 50 cells and invented the Grove Cell. 1889 saw the address of Mond, and Langer reporting on the development of Grove's work (air, not $O_2$; coal gas, not $H_2$).

In 1894 a renowned German physical chemist, Wihelm Ostwald, gave an address that stressed the thermodynamic advantages of direct electrochemical energy conversion from chemical to electrical energy and possible environmental advantages as compared with the standard method of using a steam engine and dynamo. He envisioned two pathways for the future development of technology. In the one hand, combustion engines would work inefficiently, burdened by Carnot efficiency limitations on the conversion from heat to mechanical energy, and causing the

pollution to rise to an unacceptable level. In the other, fuel cells would work efficiently, silently, and without pollution. “No Smoke, No soot, No fire”.

A more remarkable early fuel cell contribution was due to Jacques, who engineered a massive brick structure inside which there operated a cell containing an anode of carbon, while the cathode operated on air. Jacques cell functioned in molten NaOH at ~ 1V and ~100mA $cm^{-2}$ for over six months. The largest fuel cell built by Jacques in the $19^{th}$ century was a 1.5 kW system. It had a 100 cells connected externally in series.

The “Modern era of fuel cells” is generally attributed to Sir Francis T. Bacon. 1932 saw Bacon conducting fuel cell experiments as a hidden project while he worked at Parson, a well known British turbine manufacture, using high temperatures (~200°C) and high pressures (~40 atm) to reduce the polarization. The most important contribution that Bacon made was the introduction of electrodes having two layers of different pore size. The small-pore layer was in contact with the electrolyte and introduced this by capillary action to the boundary layer with the large-pored layer, filled with $H_2$ or $O_2$. Bacon was able to demonstrate a 5 kW system, which could power a 2-ton forklift. The Pratt and Whitney Aircraft bought the license to Bacon’s U.S. Patents and led to the first application of alkaline fuel cells in the Apollo space Missions.

Nerst and his student, Scottky, constructed a pseudo-fuel cell using a thin rod or tube of a high temperature (i.e. glower or lamp) of ion conducting material ($ZrO_2$ + 15%$Y_2O_3$). An electrolyte with practically the same composition used in the state of the art solid oxide fuel cell (SOFC).

Nerst also had the first ideas of redox fuel cells and for this purpose, he proposed multivalent ions of titanium, thallium, or cerium, which can be reduced or oxidized by hydrogen or oxygen.

### *1.2.2 Applications*

The Gemini Space program was the first critical application of fuel cells. Virtually every space investigation craft has had a fuel cell on board as a power source. The General Electric Company developed a solid polymer fuel cell (PEM fuel cell) for the Gemini Space missions' form 1962 to 1966. The electrolyte was a thin membrane of polystyrene sulfonic acid. The General Electric stacks had problems associated with the membrane material, polystyrene sulfonic acid becomes non-conductive after approximately 2 weeks of operation, and the extremely high catalyst loading 2 mg of platinum per square centimeter. The membrane material was replaced, in the 1970s, by a perflourinated sulfonic acid polymer (Nafion® from Dupont Chemical Company). The electron withdrawing nature of the $CF_2$ in the polymer and replacement of the C-H bonds by C-F bonds significantly enhanced the proton conductivity and the stability of the membrane. The Gemini space program was the first program to enlist the fuel cell as the main source of power for the spacecraft. The Apollo space program continued the use of fuel cells and the Space Shuttle has three 96 cell fuel cell stacks on board as its power source. The National Aeronautics Space Administration has funded the advent of fuel cells for closed systems, which are recycled and produce no waste. The fuel cell is a key participant in any type of system where a high power density is required.

### *1.2.3 System Operations*

The PEM fuel cell has many advantages over other types of fuel cells. The lack of a liquid electrolyte eliminates the corrosion and contact problems. Using a polymer eliminates the mobility of an acid electrolyte in the stack, thus the stack design is also simplified. PEM fuel

cells also have the highest power densities attainable in comparison to all other fuel cells as a result of oxygen electrode kinetics and very low Ohmic resistance in the linear region of the power density

The success of the internal combustion engine is greatly due to its range of travel and the cheap source of fuel. The long-term impact of this short-term solution has manifested itself in the air pollution over most of the major cities in the United States and abroad. A new form of energy for transportation and energy production in general is desperately required. The fuel cell, specifically the PEM fuel cell, is the most promising alternative power solution that is available. The auto industry is embracing the fuel cell as the answer to zero emission vehicles. Honda Motor Co., Nissan Motor Co., Ford Motor Co., General Motors, Toyota, and Daimler Chrysler are among the list of automobile manufactures that are researching the prospect of fuel cell power vehicles. The fuel cell has enlisted itself a clean and quiet energy source. Water is the fuel cells only obvious emission.

## 1.3 Objectives

The objectives of this research are to trace the movement of platinum in a regenerative fuel cell system and quantify the catalyst in the mobile phase. The result of the research is expected to provide data for a model the system operation and alteration in overall efficiency

## 1.4 Research Approach

To justify the existence of a “startup” condition several experiments will be carried out to quantify the immediate loss of catalyst in the fuel cell. These experiments will include a surface

rinsing, mass flux, and electrical load conditioning. The outcome of the Electrode Material Removal (EMR) and Mass Flux (MF) experiments will determine the duration of the electrical load conditions utilized for the remaining experiments. The actual catalyst losses, as measured by a Perkin-Elmer Inductively Coupled Plasma (ICP) Mass Spectrometer, will be compared against a published average particle size of the gas diffusion electrode material in an attempt to correlate the catalyst particle size against the quantity of catalyst measured.

Utilizing power production as a basis for evaluation it is possible to determine to relevance of catalyst losses as s function of the overall performance. The performance of the fuel cell is directly correlated to the amount of catalyst present and the surface area of the catalyst being utilized. The power output of the fuel cell is dependent on the active surface area of the catalyst and the physical limitations of the apparatus. Cyclic Voltammetry, which is a technique that utilizes a bipotentiostat to generate a voltage across a test cell establishing a correlation between the voltage and current in the test cell, can determine the active surface area of the catalyst. The physical limitations of the fuel cell depend on pressure, temperature, and flow rate of the fuel gases, as well as the fixture design itself. Fuel cell power output can be characterized in a power density plot, which depicts the current density vs. potential.

# 2.0 EXPERIMENTAL DESIGN

## 2.1 Proton Exchange Membrane Fuel Cell

The startup condition for the PEM fuel cell will be examined by a rinsing method, mass flux experiment and finally a timed electrical load condition.

### *2.1.1 Electrode Composition*

The gas diffusion electrode from E-TEK Incorporated, solid polymer electrolyte electrode (ELAT), will be utilized for this experimental process and throughout the thesis material. The electrode itself is constructed from three different layers. Please refer to Figure 2.

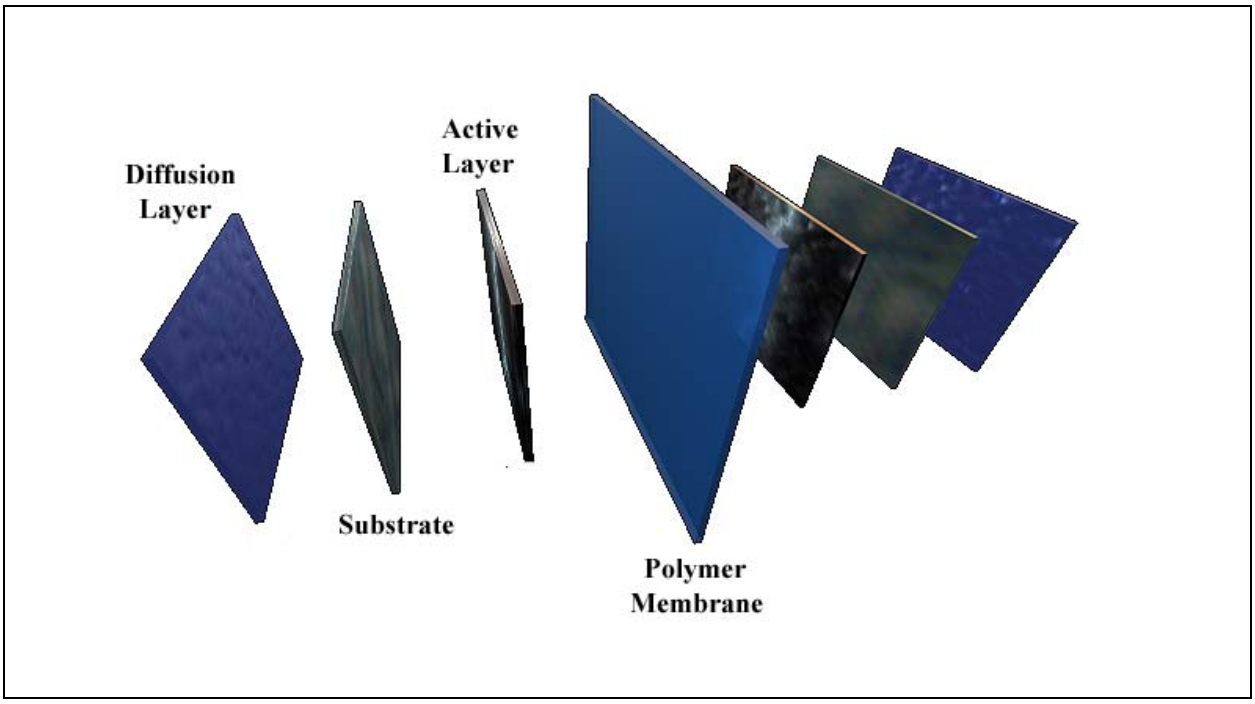


**Figure 1. Typical Membrane and Electrode Assembly**

The substrate material provides mechanical support for the electrode. ELAT electrodes have a plain carbon weave cloth of 3.4 oz/yd$^2$ with a thickness of 0.36 mm. The substrate material generally has gas-side wet proofing in the form of a hydrophobic fluorocarbon/carbon layer. The

diffusion layer is applied to the gas interface layer of the electrode, thus acting as a dispersion layer of carbon. The active layer of the electrode contains the catalyst, which has a loading determined by a specific weight of catalyst dispersed over an area. The standard loading for ELAT electrodes is 20% Pt on Vulcan XC-72 at 0.35-0.50 mg/cm$^2$. The gas diffusion electrode is then treated with an electro-catalyst, generally a tincture of the membrane material at a 5% weight, and heat treated in an oven to remove any organic compounds.

### *2.1.2 Membrane and Electrode Assemblies (MEA)*

The fuel cell itself is fabricated from a polymer membrane and two standard gas diffusion electrodes. The three components are pressed together using 2 metric tons of force at the glass transition point of the membrane material. Figure 3 is an example of the apparatus used for

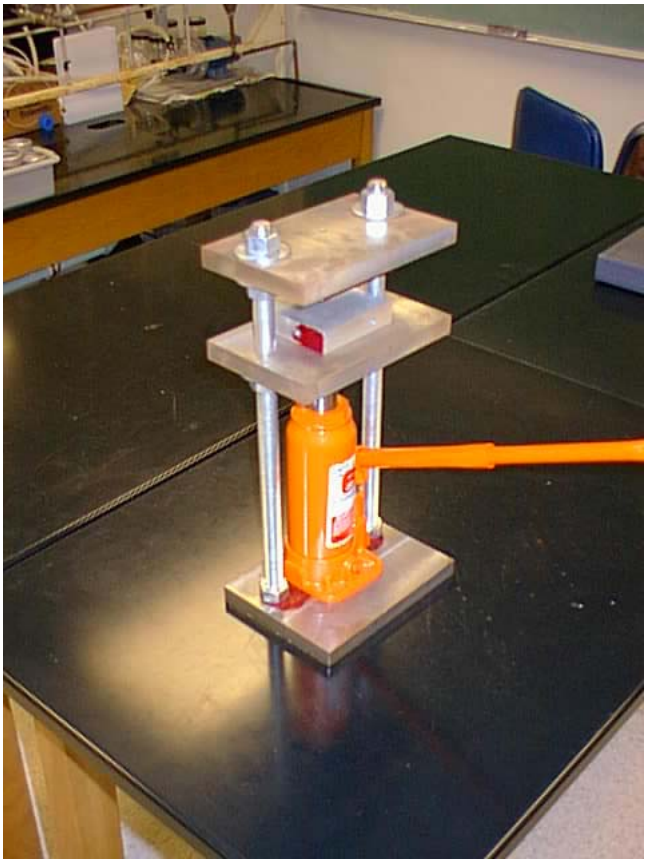

**Figure 2. Membrane and Electrode Assembly Press**

fabrication of the MEA's. The gas diffusion electrodes are held in place by gasket material and thin metal plates, insulated by a sheet of Tefzel® to prevent electrode material from adhering to the metal plate surface. The pressing procedure typically displaces some of the electrode material, thus altering the weight of the membrane and electrode assembly (MEA). Therefore the weight of the MEA components prior to pressing and after pressing will be measured.

### *2.1.3 Cyclic Voltammograms and Roughness Factors*

Cyclic Voltammetry is a procedure to quantify the active amount of catalyst. This quantity is based on the concentration of an analyte at a specific voltage, as measured by the amount of current passing through the electrolyte in question. The amount of current at a specific potential is a direct reflection of the catalyst activity, thus a proportional graphical area correlates to an active catalyst area. In order to determine the electrochemically active surface area of the electrodes, the cyclic voltammetric technique will be applied with a Pine Instrument (bipotentiostat Model AFCBP1). High purity nitrogen, humidified at the operating temperature, will be passed on the test electrode chamber. High purity Hydrogen, humidified at the operating temperature, will be passed on the counter electrode. The counter electrode will also serve as the hydrogen reference electrode.

**Typical Cyclic Voltammetry Plot**

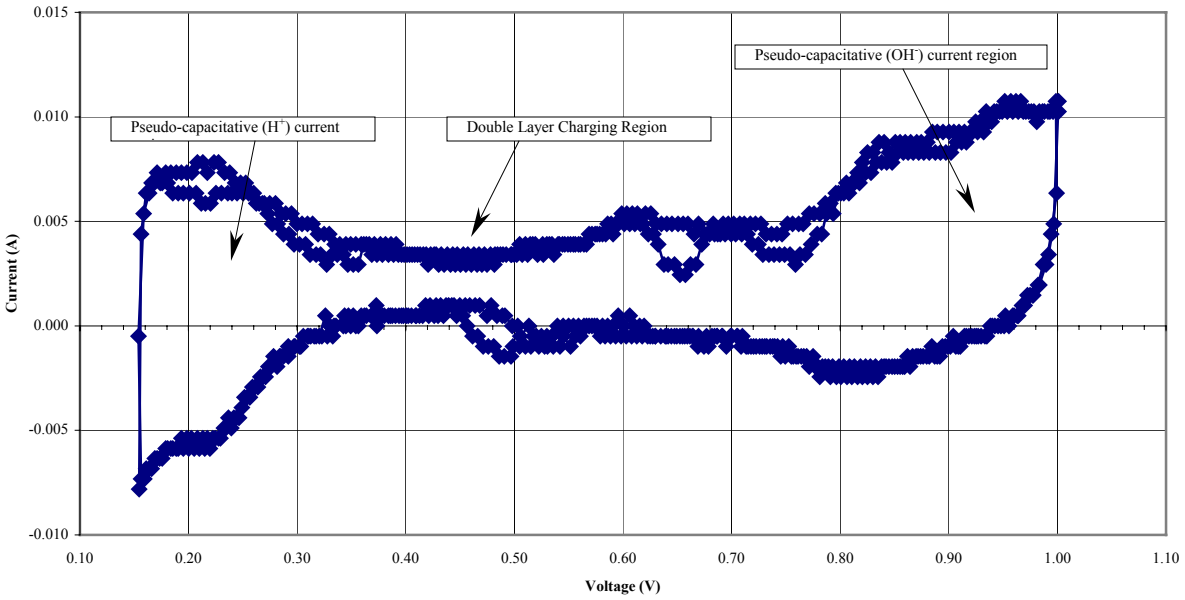


The electrochemically active surface area will be based on the columbic charge required for hydrogen adsorption or desorption on the platinum crystallites in the electrode. The amount of Faradic current measured depends directly on the analyte concentration being reduced and the rate of the sweep. The Faradic current is defined by

$$\begin{aligned} &H^+ + 2e^- \rightarrow H_2, \\ &H^+ + e^- + M \rightarrow MH_{ads}, \\ &2MH \rightarrow 2M + H_2. \end{aligned} \qquad [2.1]$$

The cyclic voltammetry sweep will be conducted from 1.00V to 0.15V, at a rate of 5 mV/Sec, for at least 10 repetitions. The pseudo-capacitative ($H^+$) current region is from a voltage of 0.15 volts to approximately 0.35 volts. In this anodic region, the reactions are governed by

$$MH_{ads} \rightarrow M + H^+ + e^-. \qquad [2.2]$$

The double layer region starts at approximately 0.35 volts and end at 0.7 volts and will be utilized to formulate the linear extrapolation required for the roughness factor. The line will be described by

$$\frac{V_A + V_B}{2} = V_X, \qquad [2.3]$$

where $V_A$ = voltage at 0.35,

$V_B$ = the minimum non-negative voltage in the double layer region,

$V_X$ = the value of the active area baseline.

The double layer region represents the balancing of the electrode charging and discharging at the analyte and solution interface. This region is assumed to have a single layer of balancing charge to the electrode and a second layer of ions balancing the analyte. The double layer region can mask the platinum hydrogen adsorption/desorption characteristics due to the redox behavior of surface active groups on carbon, i.e., quinone/hydro-quinone. This region can be skewed by additional organic contaminants complicating the masking effect of the surface active groups. In addition, if the anodic limit is extended past the 1 volt RHE, oxidation of carbon occurs. The pseudo-capacitative ($OH^-$) current region is from a voltage of 0.7 volts to approximately 1.0 volt. In this anodic region, the reactions are governed by

$$\begin{aligned} &M + H_2O \rightarrow MO + 2H^+ + 2e^-, \textit{ and} \\ &M + H_2O \rightarrow MOH + H^+ + 2e^-. \end{aligned} \qquad [2.4]$$

The comparison of the experimental area, equating to a columbic charge, and analytical loading of the catalyst will determine a "Roughness Factor". The Roughness Factor is defined by

$$\left[\frac{Experimental\ \ Area\ (\mu C)}{Surface\ \ Area\ of\ \ Electrode}\right]\left[\frac{Surface\ \ Area\ of\ \ Electrode}{220(\mu C)}\right] = Roughness\ \ Factor\,. \qquad [2.5]$$

The 220 μC corresponds to a smooth surface charge for platinum, the catalyst in this research. The ratio of the Roughness Factor and the BET surface area is described as the active surface area utilization. The assumption that the roughness factor for a smooth platinum surface is unity will be utilized.

The calculated linear area is based on a standardized linear interpolation of the raw data in the appropriate electrochemical ranges of 0.35 to 0.7 volts. The line defined by equation 2.3 will be used to determine the baseline for the experimental area calculation. The experimental area will be calculated using an integral defined by the raw data in the ranges of 0.15 to 0.35 volts.

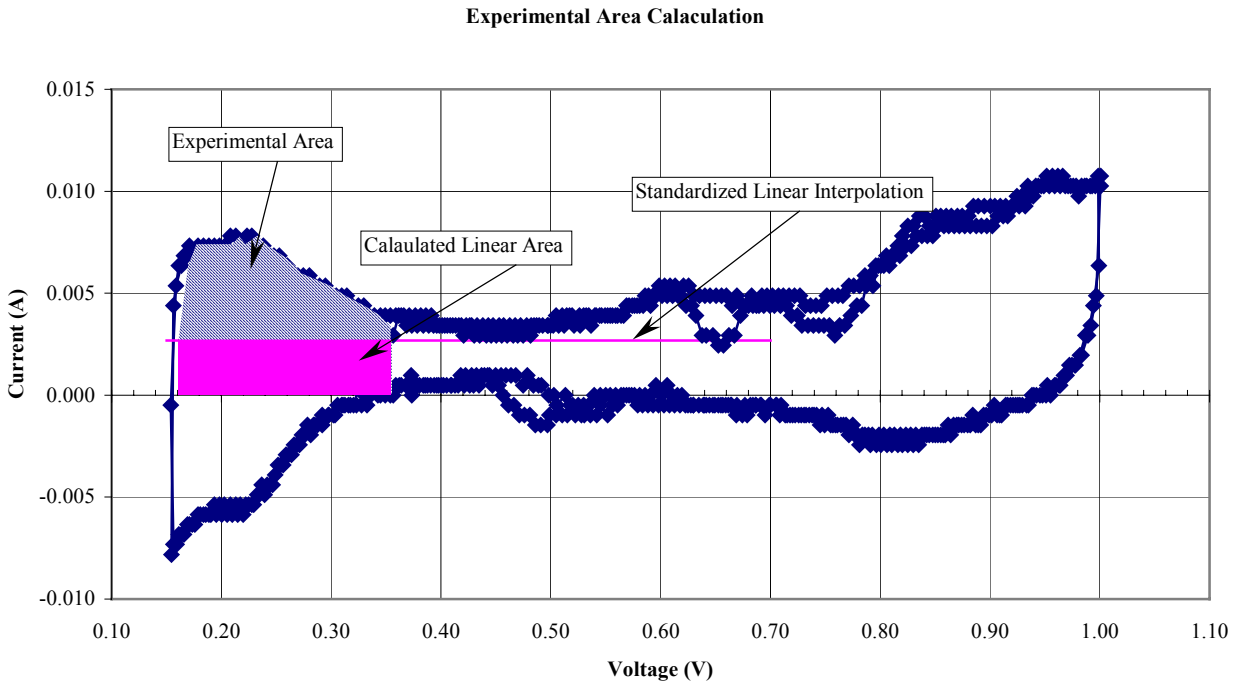


The difference between the calculated linear area and the experimental area will be utilized as the active surface area. ~~It is important to note that the experimental area goes to zero.~~

### *2.1.4 Electrode Particle Removal*

Structurally unsound electrode material displacement will be collected in a water bath. The electrode material that is collected will be analyzed by an ICP mass spectrometer for catalyst content. The content found will be utilized for the mass flow rate used in the mass flux experiment. Relatively small quantities of the catalyst will translate into a higher flow rate. The inverse of this principle will correlate to large quantities. The experiment will be carried out in an evaporation dish with the water temperature elevated to the normal operating temperature of a PEM fuel cell.

### *2.1.5 Mass Flux Experiment*

An MEA will be placed in a single cell test fixture and a peristaltic will be used to pass water through the cathodic side of the fuel cell. The water will then be collected and analyzed in a time relevant fashion with an ICP mass spectrometer. The results of this experiment will determine the amount of time necessary for the constant electrical load experiments.

### *2.1.6 Timed Operation Under a Constant Electrical Load*

Utilizing the results of the Electrode Particle Removal and Mass Flux experiments, a timed electrical load experiment will be conducted. The electrical load will consist of a carbon block variable resistance load, coupled with a multi-meter measuring the current and potential over time. The experiment will use and automatic sampling machine, controlled by a PC, to collect samples on a consistent time scale.

[Insert Pic]

### *2.1.7 Comparison of the Catalyst Losses to Particle Size*

Platinum is the standard catalyst for most PEM fuel cell systems. As the platinum loading on a carbon support increases, the platinum particles grow, thus reducing the available active surface

area of the platinum. A comparison of the average particle size of platinum on Vulcan XC-72 and the catalyst losses from the PEM fuel cell will be made. If a correlation of active surface area and particle size exists, it will be represented in the plot.

### *2.1.8 Power Density of the PEM Fuel Cell*

The power density output characteristics of a fuel cell are typically depicted in a Potential (Voltage) versus Current density graph. This graph plots the maximum current density attainable at a given set of thermal and mass flow variables. From stoichometry and half-reaction theory fuel cell should produce 1 ampere per 7cc of hydrogen at standard temperature and pressure. The calculation incorporates the following:

$$1Amp = 1C/s,$$

$$1mol\ H_2 = (2)\left(96{,}485\ \frac{C}{mol\ e^-}\right),$$

$$\left(\frac{1\ C/s}{(2)(96{,}485)}\right)(22.4)(1000)\left(\frac{60\ s}{\min}\right) = 6.964\ at\ 25^{\circ}C.$$

In practice, the equipment utilized for the experimentation must operate at approximately 100cc per minute to insure proper functionality of the fuel cell and system.

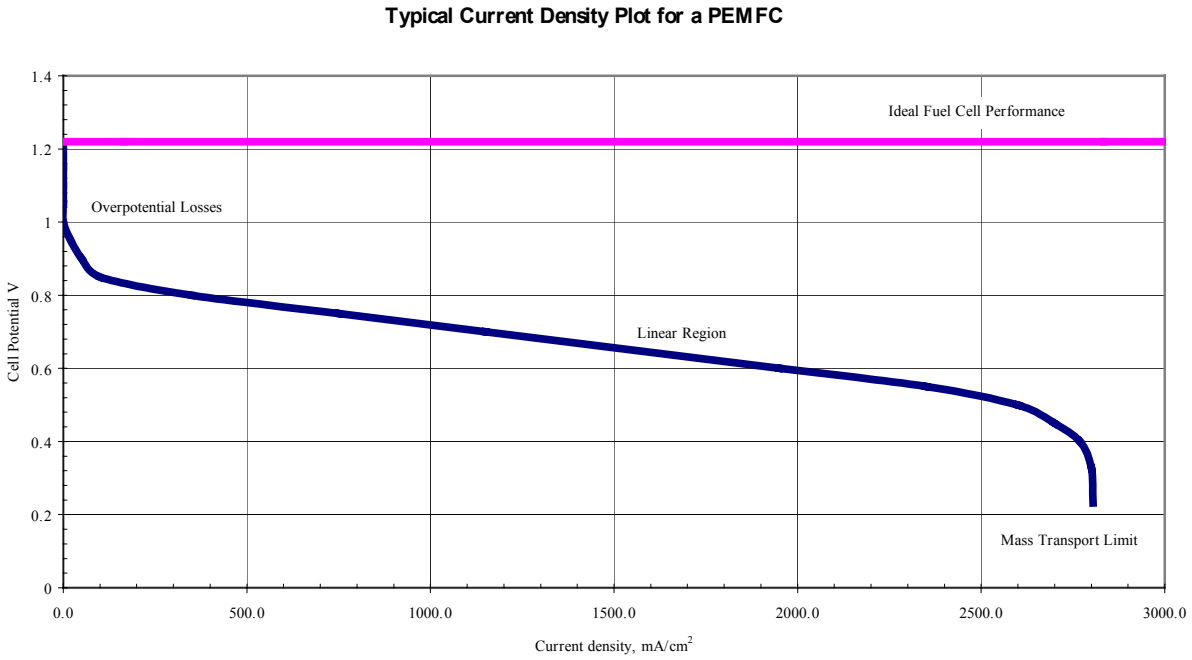


**Figure 3. Typical Current Density Plot for a PEM fuel cell**

The regions of power loss occur due to over potential, Ohmic, and mass transport limitations. Analytical observation of the initial mass and active surface area will provide the basis for evaluation of the PEM fuel cell. The use of a power density graph to establish the power consumption, which is directly related to the efficiency of the PEMWE, will be an analysis tool for the electrolysis unit.

## 2.2 Proton Exchange Membrane Water Electrolyzer

### *2.2.1 Catalyst Loading Based upon Weight*

Again cell is fabricated from a polymer membrane and two standard electrodes but the electrodes are electroplated with the catalyst, based on weight. The electrodes will be titanium wire, electroplated with platinum black. The cell components are pressed together using 2 metric tons of force at the glass transition point of the membrane material. The

### *2.2.2 Power Density of the PEM Water Electrolyzer*

The Power Density graphs plot the current consumption vs. the operation voltage, similar to a fuel cell. The graphs will be used to evaluate the power consumption, as a function of the catalyst input.

### *2.2.3 Gas Production Rates*

The production gas will be collected at a low-pressure head, and analyzed with a HP gas chromatograph. The quality of the production gas will be qualitatively assessed against a commercial sample. The possibility that the production gas may contain catalyst, although unanticipated based on physical restriction, will addressed by the analysis

# 3.0 RESULTS

## 3.1 Proton Exchange Membrane Fuel Cell

### *3.1.1 Catalyst Loading based on Weight Difference*

**Standard ETEK Electrodes**

| | Catalyst | Electrode 1 (g) | Electrode 2 (g) | Membrane (g) |
|---|---|---|---|---|
| Constant Power Low Temp 1 | 0.4 mg/cm2 | 0.1865 | 0.1747 | 0.8553 |
| Constant Power Low Temp 2 | 0.4 mg/cm2 | 0.1901 | 0.1742 | 0.9373 |
| Constant Power Low Temp 3 | 0.4 mg/cm2 | 0.2094 | 0.2053 | 1.0381 |
| Constant Power High Temp 1 | 0.4 mg/cm2 | 0.1444 | 0.1289 | 0.93 |
| Constant Power High Temp 2 | 0.4 mg/cm2 | 0.1276 | 0.1394 | 0.7435 |
| Constant Power High Temp 3 | 0.4 mg/cm2 | 0.1459 | 0.145 | 0.7939 |
| Special Load 1 | 5 mg/cm2 | 0.1442 | 0.1536 | 1.0106 |
| Special Load 2 | 5 mg/cm2 | 0.1315 | 0.1345 | 0.8385 |
| High Load 1 | Pt Black | 0.1285 | 0.1198 | 0.7238 |
| High Load 2 | Pt Black | 0.1432 | 0.1301 | 0.8638 |
| High Load 3 | Pt Black | 0.1314 | 0.1346 | 0.8716 |

| | Catalyst | Pre-Press Sum. (g) | Post-Press Total (g) | Difference (g) |
|---|---|---|---|---|
| Mass Flux 1 | 0.4 mg/cm2 | 1.3876 | 1.3826 | 0.0050 |
| Mass Flux 2 | 0.4 mg/cm2 | 1.216 | 1.2034 | 0.0126 |
| Mass Flux 3 | 0.4 mg/cm2 | 1.2222 | 1.2012 | 0.0210 |
| Constant Power Low Temp 1 | 0.4 mg/cm2 | 1.2165 | 1.1869 | 0.0296 |
| Constant Power Low Temp 2 | 0.4 mg/cm2 | 1.3016 | 1.3116 | -0.0100 |
| Constant Power Low Temp 3 | 0.4 mg/cm2 | 1.4528 | 1.41318 | 0.0396 |
| Constant Power High Temp 1 | 0.4 mg/cm2 | 1.2033 | 1.1854 | 0.0179 |
| Constant Power High Temp 2 | 0.4 mg/cm2 | 1.0105 | 0.9928 | 0.0177 |
| Constant Power High Temp 3 | 0.4 mg/cm2 | 1.0848 | 1.084 | 0.0008 |
| Special Load 1 | 5 mg/cm2 | 1.3084 | 1.2994 | 0.0090 |
| Special Load 2 | 5 mg/cm2 | 1.1045 | 1.0887 | 0.0158 |
| High Load 1 | Pt Black | 0.9721 | 0.9722 | -0.0001 |
| High Load 2 | Pt Black | 1.1371 | 1.1298 | 0.0073 |
| High Load 3 | Pt Black | 1.1376 | 1.128 | 0.0096 |

### *3.1.2 Electrode Particle Removal*

| | Concentration Mean (µg/L) | Concentration SD (µg/L) | Catalyst |
|---|---|---|---|
| MEA 1 | 14.3501 | 0.1329 | 0.4 mg/cm2 |
| MEA 2 | 14.4708 | 0.0948 | 0.4 mg/cm2 |

### *3.1.3 Mass Flux Experiment*

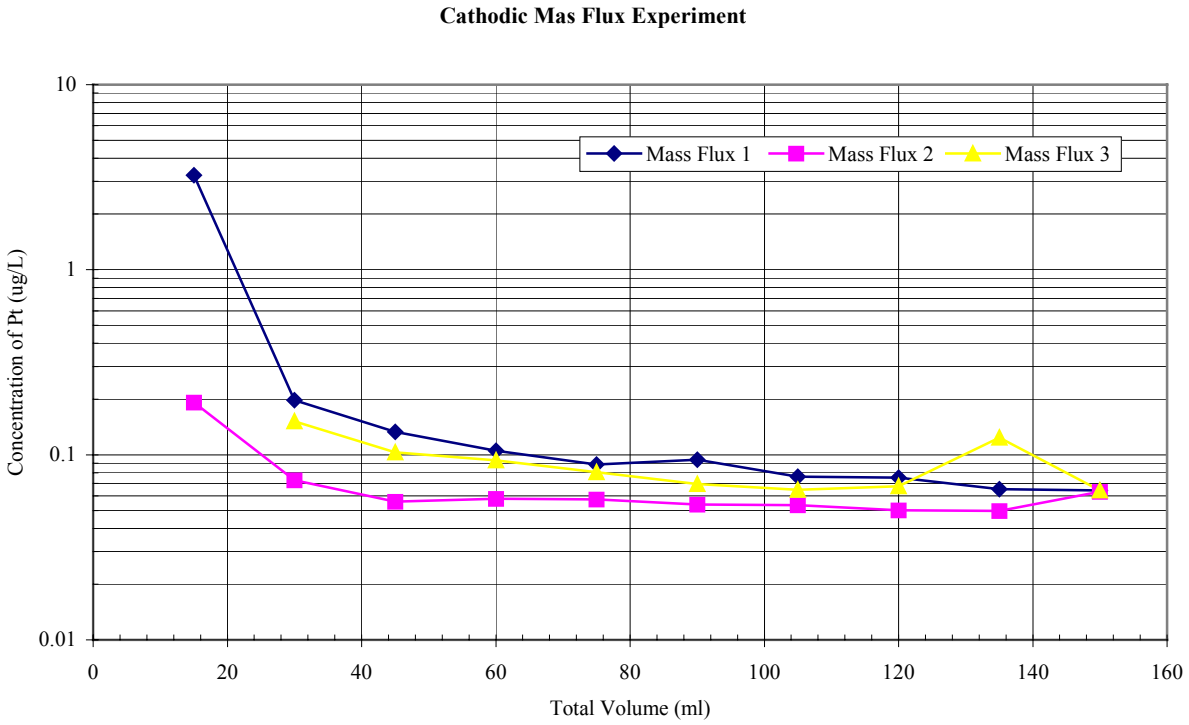


### *3.1.4 Timed Operation Under a Constant Electrical Load*

#### *3.1.4.1 Catalyst Utilization based on Cyclic Voltammetry and Power Density Plots*

These results have been grouped by MEA on a per page basis. The initial power density plot and final power density plot are on a page. The initial and final cyclic Voltammograms and experimental area calculations follow the power density graphs. The final graph

### *3.1.5 Comparison of the Catalyst Losses to Particle Size*

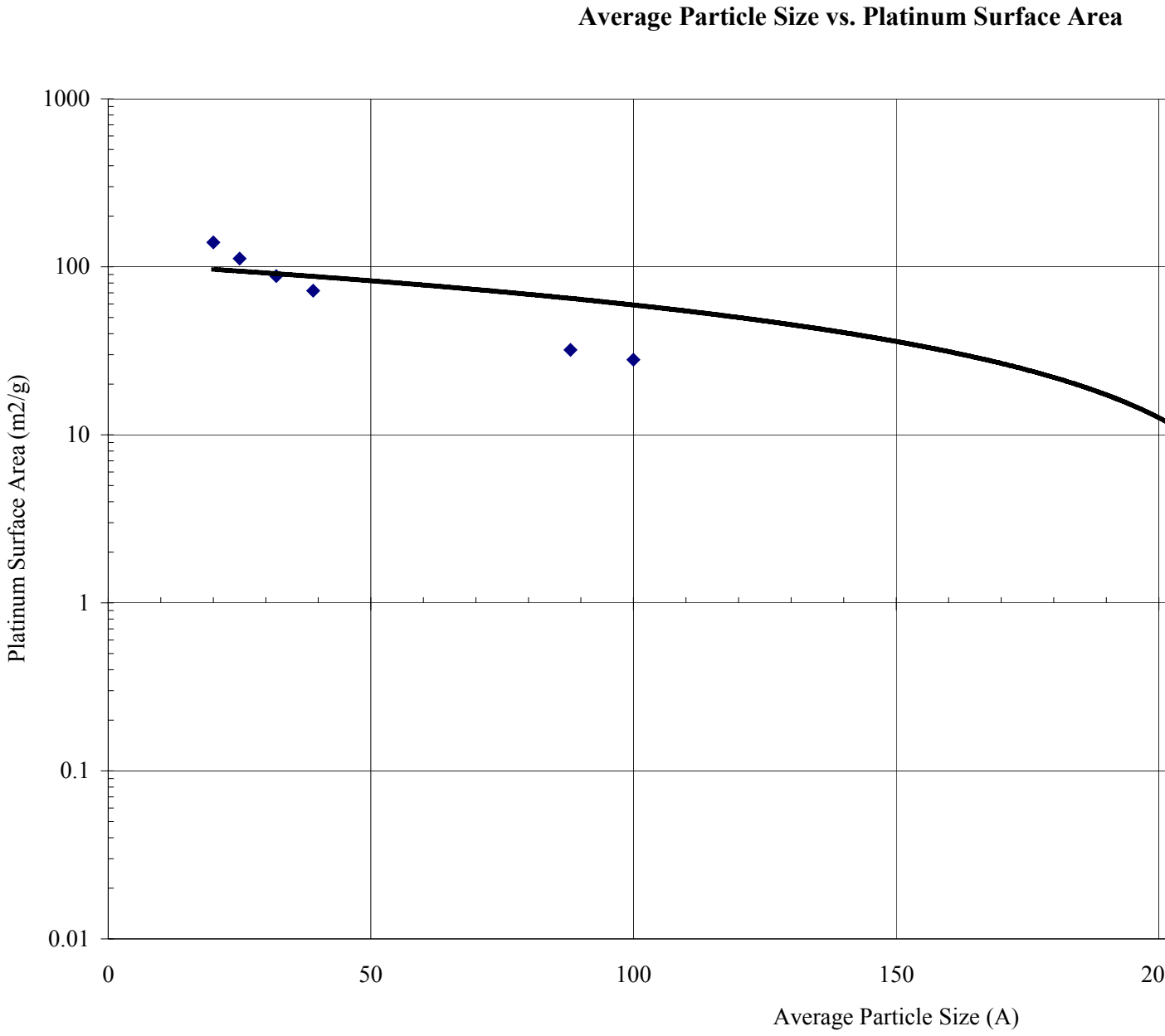


## 3.2 Proton Exchange Membrane Water Electrolyzer

### *3.2.1 Catalyst Loading based on Weight Difference*

### *3.2.2 Power Density of the PEM Water Electrolyzer*

### *3.2.3 Analysis of Product Gases*

# 4.0 ECONOMIC ANALYSIS

## 4.1 Relative Loading Losses as a Function of Catalyst Value

# 5.0 CONCLUSIONS

# REFERENCES

A.J. Appleby and F.R. Foulkes, *Fuel Cell Handbook,* Van Nostrand Reinhold, New York, 1989.

M.S. Wilson and S. Gottesfeld, *Journal of applied electrochemistry,* **22**, 1 (1992)

http://www.ballard.com

FY 1998 Contractors' Progress Report, *Development of Advanced PEM Fuel Cell Stack for Transportation Applications*

L.J.M.J. Blomen. And M.N. Mugerwa (eds.), *Fuel Cell Systems*, Plenum Press, New York, (1993)

John O'M. Bockris and Shahed U.M. Khan, *Surface Electrochemistry a Molecular Level Approach*, Plenum Press, New York, (1993)

John O'M. Bockris and Shahed U.M. Khan, *Surface Electrochemistry a Molecular Level Approach*, Plenum Press, New York, p.861 (1993)

Supraminiam Srinivasan, Renaut Mosdale, *Bulletin of Electrochemistry,* **12** (3-4), Mar-Apr. 1996, pp. 170-180

John O'M. Bockris and Shahed U.M. Khan, *Surface Electrochemistry a Molecular Level Approach*, Plenum Press, New York, p.861 (1993)

Doanh Thuc Tran, Masters Thesis, Dept. of Mechanical Engineering, Texas A&M University, College Station, TX, (1995)

Supraminiam Srinivasan, Renaut Mosdale, *Bulletin of Electrochemistry,* **12** (3-4), Mar-Apr. 1996, pp. 170-180

Pat Maio, *The Wall Street Journal*, September 13, 1999, p. R8

Supramaniam Srinivasan, Electrochemistry in transition, Plenum Press, pp.580

Sebastien Rauch, Gregory M. Morrison, Mikael Motelica-Heino, Olivier F.X. Donard, and Myriam Muris, *Elemental Association and Fingerprinting of Traffic-Related Metals in Road Sediments*, Environmental Science & Technology, **Vol. 34,** no. 15, 2000, pp. 3119-3123

# APPENDIX A

# APPENDIX B

# APPENDIX C

| | Mass Flux Experiment 1 | | | | | | |
|---|---|---|---|---|---|---|---|
| | Vial Number | Flow Rate | Pt Concentration | SD | Units | Sample Vol. (ml) | Total Vol. (ml) |
| Anodic Side | 1 | 4.0 ml/min | | | ug/L | 15 | 15 |
| | 2 | 4.0 ml/min | | | ug/L | 15 | 30 |
| | 3 | 4.0 ml/min | | | ug/L | 15 | 45 |
| | 4 | 4.0 ml/min | | | ug/L | 15 | 60 |
| | 5 | 4.0 ml/min | | | ug/L | 15 | 75 |
| | 6 | 4.0 ml/min | | | ug/L | 15 | 90 |
| | 7 | 4.0 ml/min | | | ug/L | 15 | 105 |
| | 8 | 4.0 ml/min | | | ug/L | 15 | 120 |
| | 9 | 4.0 ml/min | | | ug/L | 15 | 135 |
| | 10 | 4.0 ml/min | | | ug/L | 15 | 150 |
| Cathodic Side | 11 | 4.0 ml/min | 3.24 | 0.0816 | ug/L | 15 | 15 |
| | 12 | 4.0 ml/min | 0.197 | 0.002 | ug/L | 15 | 30 |
| | 13 | 4.0 ml/min | 0.133 | 0.00482 | ug/L | 15 | 45 |
| | 14 | 4.0 ml/min | 0.105 | 0.00372 | ug/L | 15 | 60 |
| | 15 | 4.0 ml/min | 0.0885 | 0.0064 | ug/L | 15 | 75 |
| | 16 | 4.0 ml/min | 0.0942 | 0.00746 | ug/L | 15 | 90 |
| | 17 | 4.0 ml/min | 0.0763 | 0.0048 | ug/L | 15 | 105 |
| | 18 | 4.0 ml/min | 0.0754 | 0.00488 | ug/L | 15 | 120 |
| | 19 | 4.0 ml/min | 0.0652 | 0.00423 | ug/L | 15 | 135 |
| | 20 | 4.0 ml/min | 0.0641 | 0.0059 | ug/L | 15 | 150 |

| | Mass Flux Experiment 2 | | | | | | |
|---|---|---|---|---|---|---|---|
| | Vial Number | Flow Rate | Pt Concentration | SD | Units | Sample Vol. (ml) | Total Vol. (ml) |
| Anodic Side | 1 | 4.0 ml/min | 0.707 | 0.0145 | ug/L | 15 | 15 |
| | 2 | 4.0 ml/min | 0.264 | 0.00576 | ug/L | 15 | 30 |
| | 3 | 4.0 ml/min | 0.201 | 0.00715 | ug/L | 15 | 45 |
| | 4 | 4.0 ml/min | 0.173 | 0.0082 | ug/L | 15 | 60 |
| | 5 | 4.0 ml/min | 0.171 | 0.00554 | ug/L | 15 | 75 |
| | 6 | 4.0 ml/min | 0.153 | 0.00814 | ug/L | 15 | 90 |
| | 7 | 4.0 ml/min | 0.137 | 0.00757 | ug/L | 15 | 105 |
| | 8 | 4.0 ml/min | 0.132 | 0.00525 | ug/L | 15 | 120 |
| | 9 | 4.0 ml/min | 0.124 | 0.00689 | ug/L | 15 | 135 |
| | 10 | 4.0 ml/min | 0.0641 | 0.0059 | ug/L | 15 | 150 |
| Cathodic Side | 11 | 4.0 ml/min | 0.192 | 0.0132 | ug/L | 15 | 15 |
| | 12 | 4.0 ml/min | 0.0728 | 0.00592 | ug/L | 15 | 30 |
| | 13 | 4.0 ml/min | 0.0558 | 0.00321 | ug/L | 15 | 45 |
| | 14 | 4.0 ml/min | 0.0578 | 0.00428 | ug/L | 15 | 60 |
| | 15 | 4.0 ml/min | 0.0575 | 0.00502 | ug/L | 15 | 75 |
| | 16 | 4.0 ml/min | 0.0538 | 0.00282 | ug/L | 15 | 90 |
| | 17 | 4.0 ml/min | 0.0534 | 0.00437 | ug/L | 15 | 105 |
| | 18 | 4.0 ml/min | 0.0501 | 0.00343 | ug/L | 15 | 120 |
| | 19 | 4.0 ml/min | 0.0498 | 0.00702 | ug/L | 15 | 135 |
| | 20 | 4.0 ml/min | 0.0631 | 0.00506 | ug/L | 15 | 150 |

| | Mass Flux Experiment 3 | | | | | | |
|---|---|---|---|---|---|---|---|
| | Vial Number | Flow Rate | Pt Concentration | SD | Units | Sample Vol. (ml) | Total Vol. (ml) |
| Anodic Side | 1 | 4.0 ml/min | 0.54 | 0.0175 | ug/L | 15 | 15 |
| | 2 | 4.0 ml/min | 0.139 | 0.00905 | ug/L | 15 | 30 |
| | 3 | 4.0 ml/min | 0.114 | 0.00505 | ug/L | 15 | 45 |
| | 4 | 4.0 ml/min | 0.0962 | 0.00191 | ug/L | 15 | 60 |
| | 5 | 4.0 ml/min | 0.0877 | 0.0022 | ug/L | 15 | 75 |
| | 6 | 4.0 ml/min | 0.0711 | 0.00266 | ug/L | 15 | 90 |
| | 7 | 4.0 ml/min | 0.0691 | 0.00448 | ug/L | 15 | 105 |
| | 8 | 4.0 ml/min | 0.0602 | 0.00457 | ug/L | 15 | 120 |
| | 9 | 4.0 ml/min | 0.0617 | 0.00427 | ug/L | 15 | 135 |
| | 10 | 4.0 ml/min | 0.0587 | 0.00609 | ug/L | 15 | 150 |
| Cathodic Side | 11 | 4.0 ml/min | 0.866 | 0.00617 | ug/L | 15 | 15 |
| | 12 | 4.0 ml/min | 0.152 | 0.00417 | ug/L | 15 | 30 |
| | 13 | 4.0 ml/min | 0.103 | 0.00566 | ug/L | 15 | 45 |
| | 14 | 4.0 ml/min | 0.0935 | 0.00394 | ug/L | 15 | 60 |
| | 15 | 4.0 ml/min | 0.0804 | 0.00394 | ug/L | 15 | 75 |
| | 16 | 4.0 ml/min | 0.0695 | 0.00524 | ug/L | 15 | 90 |
| | 17 | 4.0 ml/min | 0.0647 | 0.00473 | ug/L | 15 | 105 |
| | 18 | 4.0 ml/min | 0.0675 | 0.00275 | ug/L | 15 | 120 |
| | 19 | 4.0 ml/min | 0.124 | 0.00343 | ug/L | 15 | 135 |
| | 20 | 4.0 ml/min | 0.0641 | 0.0059 | ug/L | 15 | 150 |
| | 21 | 4.0 ml/min | 0.0674 | 0.00171 | ug/L | 30 | 180 |
| | 22 | 4.0 ml/min | 0.0524 | 0.00733 | ug/L | 30 | 210 |
| | 23 | 4.0 ml/min | 0.057 | 0.00526 | ug/L | 30 | 240 |
| | 24 | 4.0 ml/min | 0.0503 | 0.00171 | ug/L | 30 | 270 |
| | 25 | 4.0 ml/min | 0.0494 | 0.0023 | ug/L | 30 | 300 |
| | 26 | 4.0 ml/min | 0.0484 | 0.00533 | ug/L | 30 | 330 |
| | 27 | 4.0 ml/min | 0.0563 | 0.00516 | ug/L | 30 | 360 |
| | 28 | 4.0 ml/min | 0.206 | 0.00113 | ug/L | 30 | 390 |
| | 29 | 4.0 ml/min | 0.06 | 0.00287 | ug/L | 30 | 420 |
| | 30 | 4.0 ml/min | 0.0569 | 0.00296 | ug/L | 30 | 450 |
| | 31 | 4.0 ml/min | 0.0484 | 0.00297 | ug/L | 30 | 480 |
| | 32 | 4.0 ml/min | 0.043 | 0.00176 | ug/L | 30 | 510 |

| *Vial Number* | *Sample Volume (ml)* | *Pt Concentration (ug/L)* | *Plasma SD* | *Temp (C)* | *Area Correction* |
|---|---|---|---|---|---|
| CPL-3 | 11.75 | 6.1201 | 0.0165 | 75 | 12.2402 |
| CPH-1 | 12.5 | 2.9373 | 0.0405 | 30 | 5.8746 |
| CPH-2 | 12.5 | 3.3235 | 0.0141 | 30 | 6.647 |
| CPH-3 | 12.5 | 3.1077 | 0.0704 | 30 | 6.2154 |
| PB-1 | 12.5 | 8.2583 | 0.1286 | 50 | 16.5166 |
| PB-2 | 12.5 | 5.0836 | 0.056 | 50 | 10.1672 |
| PB-3 | 12.6 | 5.2102 | 0.0502 | 50 | 10.4204 |
| SL-1 | 12.5 | 3.6427 | 0.0232 | 50 | 7.2854 |
| SL-2 | 12.5 | 3.5676 | 0.0794 | 50 | 7.1352 |
| MEA-1 | 500 | 14.3501 | 0.1329 | 75 | 14.3501 |
| MEA-2 | 500 | 14.4708 | 0.0948 | 75 | 14.4708 |